iScience

CellPress
OPEN ACCESS

Review

Metal-organic frameworks for high-performance cathodes in batteries

Jeongmin Lee,[1,2] Inyoung Choi,[1,2] Eunji Kim,[1,2] Junghyun Park,[1,2] and Kwan Woo Nam[1,*]

SUMMARY

Metal-organic frameworks (MOFs) are functional materials that are proving to be indispensable for the development of next-generation batteries. The porosity, crystallinity, and abundance of active sites in MOFs, which can be tuned by selecting the appropriate transition metal/organic linker combination, enable MOFs to meet the performance requirements for cathode materials in batteries. Recent studies on the use of MOFs in cathodes have verified their high durability, cyclability, and capacity thus demonstrating the huge potential of MOFs as high-performance cathode materials. However, to keep pace with the rapid growth of the battery industry, several challenges hindering the development of MOF-based cathode materials need to be overcome. This review analyzes current applications of MOFs to commercially available lithium-ion batteries as well as advanced batteries still in the research stage. This review provides a comprehensive outlook on the progress and potential of MOF cathodes in meeting the performance requirements of the future battery industry.

INTRODUCTION

As the use of fossil fuels increases along with industrial development, greenhouse gas emissions, such as carbon dioxide generated during fuel combustion, are increasing.[1] High concentrations of greenhouse gases in the atmosphere are the main cause of global warming and various ecosystem disturbances. Accordingly, the international community is focusing on clean energy for net zero carbon, and the demand for batteries for storing the electrical energy produced from renewable energy sources is increasing.[2] Batteries are used in a diverse range of products such as portable electronic devices and electric vehicles (EVs) and their range of applications is still expanding.[3–5] Thus, numerous studies are being carried out to improve battery performance for new and growing applications. Among them, the development of novel, efficient, and cost-effective electrode materials occupies an important position in the goal of improving battery performance.[6]

The overall performance and price of the battery are primarily dictated by the cathode.[7–9] Therefore, cathode active materials play an important role in the development of metal-ion rechargeable batteries and researchers continue to develop optimal cathode active materials to improve battery performance.[10] The cathode active material should be able to reversibly intercalate/deintercalate a large number of metal cations in order to increase the energy efficiency in the charging and discharging process.[11] In addition, it is necessary to meet the required high volumetric capacity and specific capacity through a light and compact structure, and to produce high output performance by increasing both electrical and ionic conductivity. To eliminate reactions with electrolytes and other minor materials, they must be electrochemically or thermally stable. However, the cathode materials developed so far have limited capacity, power performance, and cycle-life characteristics and are not ideal for high-performance applications such as EVs. Moreover, there are many challenges that need to be solved to extend the durability of batteries. Specifically, composite materials and structures that preserve the crystallinity without disrupting the intercalation/deintercalation of carrier ions in the host cathode need to be developed. Also, the relatively low electrical conductivity of Metal-organic framework (MOF) is one of the biggest problems to be solved.

MOFs have crystalline structures with high porosity consisted of transition metal center and an organic linker.[12,13] As shown in Figure 1, the chemical properties, surface area, and pore size of the synthesized MOF are dependent on the combination of transition metals and organic linkers selected.[14–16] The tunable characteristics of MOFs make them suitable for supercapacitors[17–19] and rechargeable batteries.[20] In addition, MOF-derived structures provide a robust framework that can withstand the physical impacts that occur during metal cation insertion and deintercalation processes.[21]

Electrical transport in MOFs can be activated by two approaches, so-called through-bond and through-space strategies. The through-bond approach emphasizes enhancing the bond strength between the metal and ligands for increased charge dispersion, while the through-space approach concentrates on non-covalent interactions among organic fragments, specifically $\pi - \pi$ stacking, to establish uninterrupted pathways for charge transfer. These pathways could influence the transport properties of MOFs.[22]

[1]Department of Chemical Engineering and Materials Science, and Graduate Program in System Health Science and Engineering, Ewha Womans University, Seoul 03760, Republic of Korea
[2]These authors contributed equally
*Correspondence: kwanwoo@ewha.ac.kr
https://doi.org/10.1016/j.isci.2024.110211

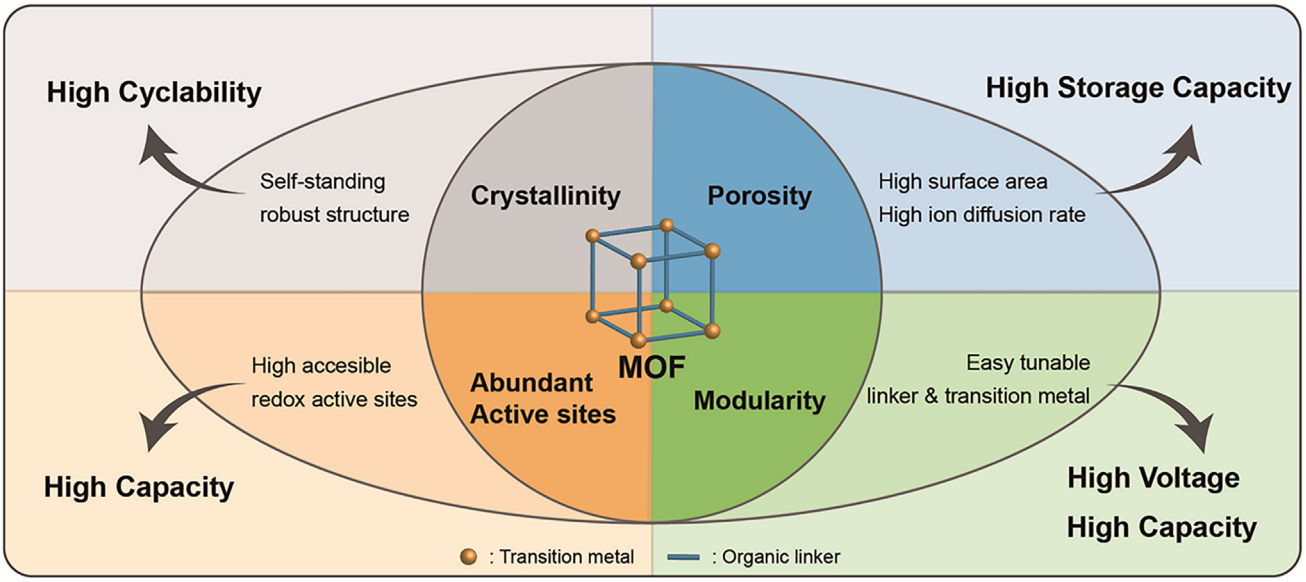

Figure 1. Advantages of MOF as a battery cathode material

Advantages of MOF materials suitable for battery cathodes materials: crystallinity, porosity, abundant active sites, and modularity.

In general, for lithium-ion batteries (LIBs), the cathode refers to a compound consisting of an active material, a conductive agent, and a binder coated with an aluminum current collector. In this paper, cathodes using redox-active MOF materials for metal-ion batteries, MOF composites with a sulfur active material for lithium-sulfur batteries (LSBs), and MOF catalysts for oxygen reduction in metal-air batteries are reviewed. This review classifies MOF-based cathodes according to the type of battery and analyzes the performance, advantages, and limitations of cathodes with MOF-derived materials. This review highlights the potential of MOFs as active cathode materials for the future instruction of rechargeable batteries.

METAL-ORGANIC FRAMEWORK CATHODES IN METAL-ION BATTERIES

Metal-ion batteries, such as the widely used LIBs and the advanced aqueous rechargeable zinc-ion batteries (ZIBs), produce and store electrical energy through a redox reaction according to the insertion and deinsertion process of metal ions moving in the cathode structure. Among the battery components, the cathode determines the overall performance of the cell, specifically the capacity, voltage, and lifespan characteristics.[23] Therefore, it is important to develop a cathode material that can achieve a high energy density while exhibiting high power performance and long cycle-life properties.[24,25] In general, it is possible to improve the energy density of the battery by increasing the output voltage or capacity of the cathode material.

However, with the existing cathode materials, if the output voltage or capacity is increased to improve the energy density of the cathode material, structural collapse of the cathode inevitably occurs, causing problems such as capacity fading or deterioration of safety.[7,26,27] Transition metal oxides have sufficient stability of host structure in the process of the metal ion intercalation/deintercalation to the cathode in the energy density range required for current LIBs.[28–32] However, for cathode materials in rechargeable batteries used in EVs, a higher energy density is required, which causes the structural collapse of current cathode materials.[33] Current solutions involve forming an insulating metal oxide at the interface, which acts as a high-potential barrier and results in a decrease in capacity. In addition, the bulk phase of the active material lacks an efficient diffusion path for metal ions, leading to incomplete intercalation/deintercalation.[34] Therefore, research about developing a completely new class of cathode active materials is needed.

MOF cathode materials have received considerable attention owing to their flexible design potential. They can form numerous structures according to the type of transition metal and organic linker used. Furthermore, MOFs[35] can have high crystallinity, high stability, and their porous and conjugated electronic structure that allows high ionic/electrical conductivity in Figure 1. In addition, it is possible to increase redox activity[36,37] in Figure 1 by creating abundant redox sites through open metal sites. Figure 2 shows the MOF redox mechanism at the transition metal sites, and the organic linkers and the pore structure that allows ions and oxygen to penetrate. To use MOFs as cathodes in metal-ion batteries, studies are being conducted to compensate for their shortcomings while exploiting the advantages of MOFs.

In this section, we classify MOFs based on two battery type applications, LIBs and ZIBs, and analyze the capacity and cyclability of the MOF cathode materials. Then, directions for future research that will allow MOFs to be introduced into the cathode more effectively are suggested.

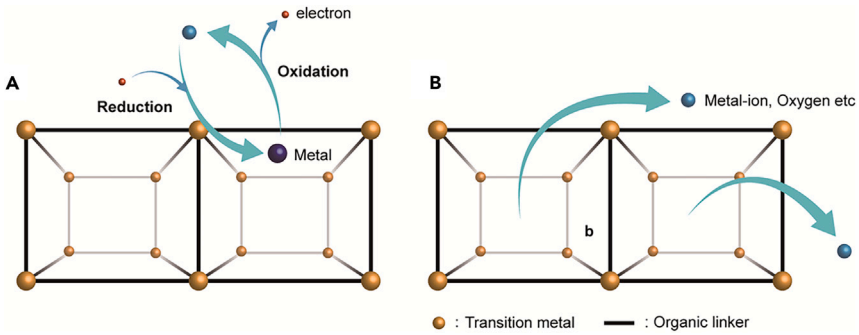

Figure 2. Redox mechanism of MOF as a battery cathode

(A) The redox mechanism of MOF.

(B) Movement of metal-ions and oxygen in the MOF pore structure.

Metal-organic framework cathodes in lithium-ion batteries

LIBs have been the most commercialized type of rechargeable batteries for several decades owing to their long cycling stability and high energy density.[38] With the commercialization of EVs, research is being actively conducted to increase the capacity and lifespan of LIBs. However, the currently used layered transition metal oxide (TMO)-based cathodes have a relatively low capacity (<200 mAh g^{-1}) and exhibit rapid degradation of cell performance.[39] MOFs that have high porosity,[40] abundant redox-active sites,[41] and rigid[42] extended frameworks can overcome these disadvantages. Especially, two-dimensional (2D) MOFs have high conductivity by strengthening the electron distribution due to extended conjugation of π-d orbitals between the organic linker and the metal node in the plane.[22] In addition, through-space transport of electrons contributes to the enhanced conductivity of 2D MOF.[43,44] (Figure 3) Detailed capacities of LIB MOF cathodes are provided in Table 1.

Jiang et al. used[44] an active 2D copper-benzoquinoid MOF (Cu-THQ MOF) (electrical conductivities of 2.15x10^{-3} to 0.16 uS cm^{-1} depending on temperature from 30 to 110 °C)[45] as a cathode active material and showed a high reversible capacity (>350 mAh g^{-1}), high gravimetric energy density (775 Wh kg^{-1}), and good cyclability. Both the transition metal ions and the organic linkers of the 2D Cu-THQ MOF showed good redox activity during the charge and discharge processes as well as high porosity, and the 2D conjugate structure of the 2D Cu-THQ MOF improved the battery performance. Cai et al. synthesized[46] 2D Fe-DHBQ (electrical conductivity of 1.1x10^{-4} S cm^{-1}) as a cathode active material using 2,5-dihydroxybenxoquinone linker and it showed a high capacity of 346 mAh g^{-1} at 50 mA g^{-1}. In particular, it provided a high capacity of 237 mAh g^{-1} even under practical battery conditions with electrode composition (active material: binder: conductive agent = 8:1:1) and high mass loading of 12 mg cm^{-2}. Peng et al. applied[47] a triphenylamine-based Cu-TCA MOF as a cathode active material. It has a porous structure with a pore radius of 1 nm and abundant redox-active sites. The redox activities of Cu^{2+} ions located at the metal ion sites and N atoms bonded to three adjacent benzene rings in the organic linkers enable a theoretical capacity of 145 mAh g^{-1} at 31.6 mA g^{-1}. In addition, they suggested that the high porosity of the Cu-TCA MOF could maintain a high-rate capability without capacity fading. Zhang et al. utilized[48] a microporous redox-active MOF, Cu(2,7-AQDC)(2,7-H_2AQDX = 2,7-anthraquinone carboxylic acid) as a cathode active material, with a voltage window of 1.7–4.0 V, and both metal ions and linkers of the Cu(2,7-AQDC) MOF exhibited redox activity.

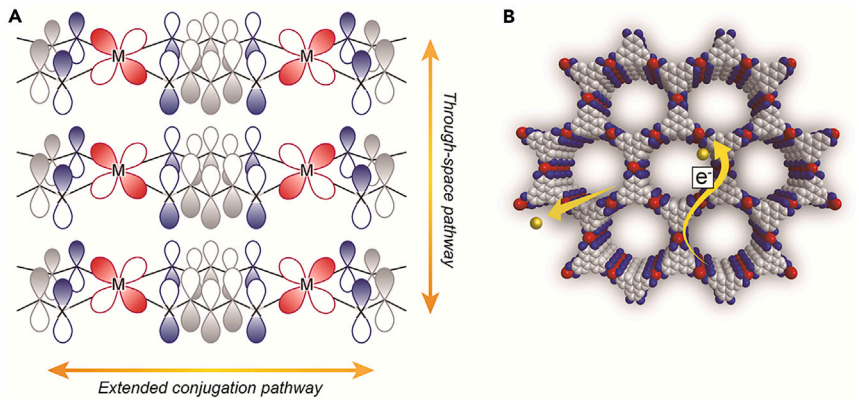

Figure 3. Conductive mechanism of 2D MOF

(A) Orbital schematic for potential charge transport pathways in 2D MOFs.

(B) Schematic diagram for the in-plane and out-of-plane conduction of electrons in 2D MOFs.

Table 1. Performance comparison of MOF cathodes applied to each battery system

MOFs	Sample	Rate (C or mA g^{-1})	Reversible Capacity (mA h/g)	Cycle number	Reference
Li-ion batteries					
Cu-THQ	Cu-THQ	50 mA g^{-1}	387	2	Jiang et al.[45]
Fe-DHBQ	Fe-DHBQ	50 mA g^{-1}	346	1	Cai et al.[46]
Cu-TCA	Cu-TCA	31.6 mA g^{-1}	102.2	1	Peng et al.[47]
Cu(2,7-AQDC)	Cu(2,7-AQDC)	0.1 C	105	50	Zhang et al.[48]
MIL-101	Fe-MIL-101	0.005 C	107	1	Yamada et al.[49]
$Fe_2(DFc)_3$	$Fe_2(DFc)_3$	50 mA g^{-1}	172	5	Li et al.[50]
Fe-TABQ	Fe-TABQ	50 mA g^{-1}	268.8	1	Geng et al.[51]
Mn-DMA	Mn-DMA	0.005 C	205	1	Zhang et al.[52]
MIL-53	Fe-MIL-53	0.1 C	70	50	Férey et al.[53]
Cu-CuPc	Cu-CuPc	0.04 C	128	1	Nagatomi et al.[54]
BTC	Li-Co-BTC	50 mA g^{-1}	155.6	50	Du et al.[55]
Zn-ion batteries					
$Cu_3(HHTP)_2$	$Cu_3(HHTP)_2$	50 mA g^{-1}	228	1	Nam et al.[63]
$Cu_3(HHTP)_2$	$Cu_3(HHTP)_2$	400 mA g^{-1}	166.9	1000	Wang et al.[64]
MIL-47	V-MIL-47	100 mA g^{-1}	332	1	Ru et al.[65]
MIL-100	MIL-100(V)	200 mA g^{-1}	362	1	Mondal et al.[67]
Mn(BTC)	$Fe_2(DFc)_3$	100 mA g^{-1}	138	1	Pu et al.[68]
BTA	Cu-BTA	200 mA g^{-1}	330	1	Sang et al.[71]
Li-air batteries					
MOF-74	MnCo-MOF-74	50 mA g^{-1}	387	2	Kim et al.[84]
MOF-74	Co-MOF-74-X	100 mA g^{-1}	11,350	1	Yan et al.[85]
Mn-MOF	2D-Mn-MOF	1,000 mA g^{-1}	9,464	1	Yuan et al.[86]
Ni(4,4-bipy)(H_3BTC)	Ni(4,4-bipy)(H_3BTC)	0.12 mA cm^{-2}	9,000	1	Hu et al.[87]
MOF-74	Mn-MOF-74	50 mA g^{-1}	9420	1	Wu et al.[88]
MOF-74	Tz-Mg-MOF-74	50 mA g^{-1}	7700	1	Li et al.[89]
Li-S batteries					
Cu-TDPAT	Cu-TDPAT	1675 mA g^{-1}	745	500	Hong et al.[124]
Cu-H3BTC	Cu-H3BTC	200 mA g^{-1}	1051.3	300	Feng et al.[125]
MOF-525	MOF-525(Cu)	325 mA g^{-1}	700	200	Wang et al.[126]
MOF-TOC	MOF-TOC	1675 mA g^{-1}	964	1	Zeng et al.[127]
DS-MOF	1D-DS-Co-MOF	200 mA g^{-1}	191	1	Shimizu et al.[128]
DS-MOF	2D-DS-Cu-MOF	200 mA g^{-1}	175	1	Shimizu et al.[128]
DS-MOF	3D-DS-Mn-MOF	200 mA g^{-1}	160	1	Shimizu et al.[128]
UIO66	CNT@UIO66-S	1675 mA g^{-1}	608	450	Liu et al.[129]

Fe is one of the most inexpensive and sustainable metal elements, and its Fe^{2+}/Fe^{3+} mixed valence characteristics can result in high electrical conductivity and additional capacity,[46] so it has been frequently used as a metal node for MOF cathodes. Yamada et al. investigated[49] Fe-MIL-101 MOF as a cathode active material for LIBs, which has low cost but moderate activity. The Fe-MIL-101 MOF has a rigid framework with a three-dimensional (3D) microporous structure composed of large pore sizes around 12 to 15 Å. This cathode showed good cyclability over 100 cycles and high coulombic efficiency due to the robust structure of the active material, which minimizes side reactions with the electrolyte. Li et al. successfully synthesized[50] Fe (III) 1,1-ferrocenedicarboxylic ($Fe_2(DFc)_3$) as a cathode material for LIBs. During the charge and discharge processes, the redox reaction of Fe ions proceeded well, while the guest PF_6^- anion intercalated into the $Fe_2(DFc)_3$ host. This Fe-based MOF exhibited a high discharge capacity of 172 mAh g^{-1} at 50 mA g^{-1} and a high operating potential of 3.55 V due to its stable structure during battery cycling. Similarly, Fe-tetraamino-benzoquinone (Fe-TABQ), which has a 2D structure and dual redox active units, has also been applied as a cathode.[51] Robust Fe-N/Fe-O bonds were formed by strong π-d orbital interactions between Fe metal nodes and TABQ

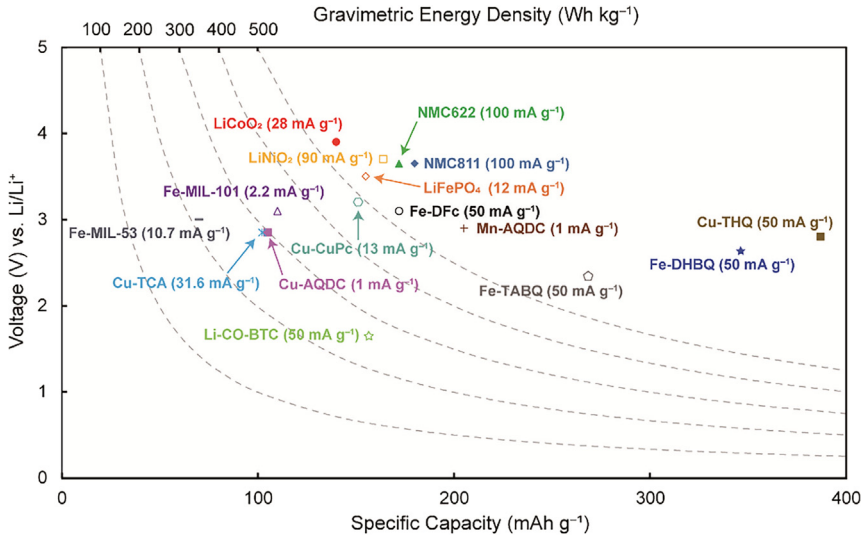

Figure 4. Operation voltage versus specific capacities of lithium-ion battery electrode materials
Comparison of performance between various MOF cathodes and representative commercial cathode materials in LIBs.[44–59]

ligands, resulting in excellent electrochemical stability. Thus, it achieved a capacity of 268.8 mAh g^{-1} at 50 mA g^{-1} and showed good cyclability by maintaining more than 95% of its initial capacity over 200 cycles.

Zhang et al. reported[52] on the electrochemical mechanism called "bipolar charging." They used a Mn-DMA MOF (DMA = N,N-dimethylacetamide) as a cathode active material and showed the intercalation of PF_6^- anions into the framework during the charging process, which were released during the discharging process, followed by Li^+ ion insertion. This mechanism is possible because of the large pore size of Mn-DMA MOF. Férey et al. used[53] Fe-MIL-53 MOF with one-dimensional (1D) diamond-shaped channels, and Nagatomi et al. applied[54] Cu-CuPc MOF (electrical conductivities ranging from 9.4×10^{-8} to 1.6×10^{-6} S cm^{-1}) with a hierarchical micro/mesoporous structure. Du et al. synthesized[55] two ternary Li-Co-BTC MOFs constructed using Co/Li metal sites and 1,3,5-benzenetricarboxylic acid (H_3BTC). During the charge-discharge process, the 1D channel in Li-Co-BTC improved the diffusion rate of Li^+ ions and electrolyte penetrability. Figure 4 shows the average voltage and capacity of the MOF cathode materials mentioned in the text and representative cathode materials in current LIBs in one graph.

Metal-organic framework cathodes in zinc-ion batteries

Aqueous rechargeable ZIBs are likely to replace LIBs for the large-scale ESSs because of their high safety, large capacity, low cost, excellent ionic conductivity, good rate capability, and the proper redox potential of Zn (– 0.76 V vs. standard hydrogen electrode) which can be driven reversibly in aqueous electrolytes.[56,57] Several types of cathode materials for aqueous rechargeable ZIBs have been studied, such as manganese-based cathodes,[58–60] vanadium-based cathodes,[61] and quinone.[62] However, these cathodes face several challenges such as rapid capacity fading, serious toxicity, poor rate performance, and dissolution issues during cycling. Specific experimental capacities of ZIB MOF cathodes are listed in Table 1.

Nam et al. employed[63] $Cu_3(HHTP)_2$ (HHTP = 2,3,6,7,10,11-hexahydroxy-triphenelyene) (electrical conductivity of 0.2 S cm^{-1}) as a cathode active material for aqueous rechargeable ZIBs. Cu-HHTP has stacked π-conjugated 2D conductive layers, with large 1D channels, which store Zn^{2+} ions and exhibit a high diffusion rate as well as low interfacial resistance. In addition, both copper and quinoids in Cu-HHTP act as redox-active sites, increasing the theoretical capacity of the Cu-HHTP cathode. This results in a remarkable reversible capacity (228 mAh g^{-1}) and high-rate capability. Following this research, a MOF-based cathode composed of Cu-HHTP and MXene was investigated.[64] Cu-HHTP/Mxene forms a sandwich-like heterostructure, and this structural characteristic alleviates the aggregation of Cu-HHTP nanosheets during charge-discharge. Additionally, Cu-HHTP/Mxene provides more abundant active sites and a wider contact area to promote the transfer rate of Zn^{2+} ions than Cu-HHTP. This cathode showed a specific capacity of 170.6 mAh g^{-1} at a rate of 4 A g^{-1} and 166.9 mAh g^{-1} was retained after 1000 cycles, thereby exhibiting outstanding cyclability. Ru et al. synthesized[65] typical V-MIL-47 MOFs using vanadium (V) as the metal cluster and 1,4-benzenedicarboxylate (bdc) as the organic ligand. V-MIL-47 MOF has a 1D layered structure with high conductivity and hierarchical porosity. (MIL-47 powder has 243 mS cm^{-1}, increased by V[66]) Such a rigid structure with abundant redox-active sites is favorable for long cycle durability and high capacity. In addition, owing to its highly open structure, V-MIL-47 enhances the rate of Zn^{2+} ions and improves the electrical conductivity; thus, the electrochemical performance of V-MIL-47 MOF displays a high-rate capability, cycling performance, and initial specific capacity of 332 mAh g^{-1} at a current rate of 100 mA g^{-1}. Similarly, Mondal et al. applied[67] V-based MOF with a 3D structure as a cathode. MIL-100 (V) was synthesized, which is composed of V as metal node and triethyl-1,3,5-benzenetricarboxylate as the organic ligand. MIL-100 (V) has two different sizes of mesoporous cages by having 3D

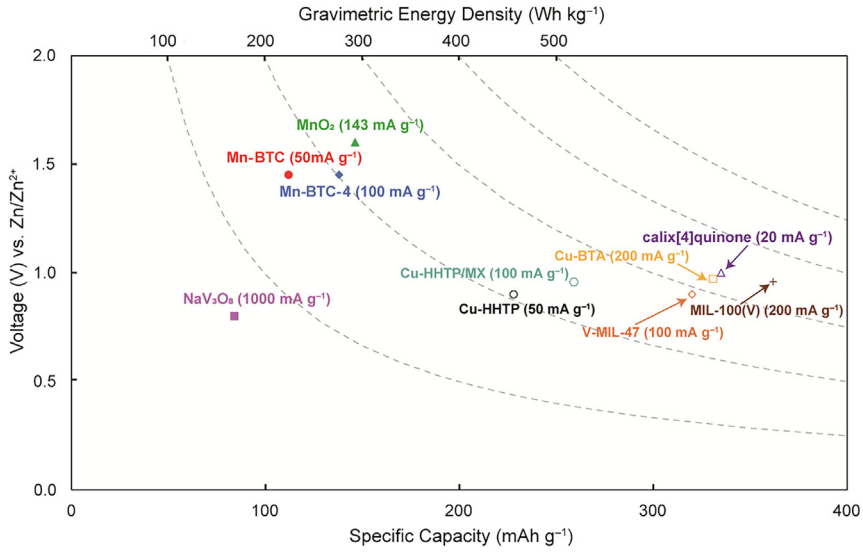

Figure 5. Operation voltage versus specific capacities of aqueous rechargeable zinc-ion battery electrode materials
Comparison of performance of MOF cathodes and other representative cathodes for aqueous rechargeable ZIBs.[63–73]

zeolite construction. Thus, transport of Zn^{2+} ion was facilitated, and the accessible active sites were increased. Therefore, it showed a high capacity of 362 mAh g^{-1} at 0.2 A g^{-1}.

Pu et al. used[68] Mn(BTC) that is composed of Mn ions and trimesic acid (H_3BTC = 1,3,5-benzenetricarboxylic acid) that forms a 3D network as a cathode active material. (Electrical conductivity of 2.3 mS cm^{-1} for polymer (PEO-CLP) composite.[69]) Although the Mn ion in the Mn(BTC)-MOF is a redox-active center during the Zn storage process, BTC turned out to be a redox-inactive ligand. The charge storage mechanism for Mn(BTC)-MOF involves two steps. The first is the formation of Zn(BTC)-MOF through the translocation of manganese ions and zinc ions during battery operation. The second step is the formation of MnO_2 by the oxidation of Mn ions. Yin et al. also used[70] coordinately unsaturated Mn-BTC with different coordination degrees (molar ratios of Mn and -COOH were 1:2, 1:4, and 1:6, respectively). Among the three samples, Mn-BTC with a molar ratio of Mn to COOH of 1:4 showed the highest capacity of 138 mAh g^{-1} at a rate of 100 mA g^{-1}, which dramatically improved its inherent activity and structural stability. Their good stability is a result of strong hydrogen bonding and π–π interactions. Sang et al. maximized redox activity of MOF cathode by adopting an ultrasmall 1,2,4,5-benzenetetramine (BTA) as organic ligand.[71] In this study, the electrochemical tests were conducted on Ni-BTA and Cu-BTA cathode and Cu-BTA exhibited better performance due to its dual redox mechanism of the Cu metal node and BTA ligand. Thus, Cu-BTA provided a capacity of 330 mAh g^{-1} at 0.2 A g^{-1}, while Ni-BTA showed a capacity of 200 mAh g^{-1}. These results demonstrate how important the combination of metal node and organic ligand is when using MOF as a cathode.

The porous structure and conductivity of MOFs are beneficial to their ion and electron transfer abilities, thereby improving the rate capability and cyclability of the cathode. Finally, the average voltage and capacity between the MOF cathodes and other representative cathodes for aqueous rechargeable ZIBs are compared in Figure 5.

The roles of various transition metals in MOF-based cathodes are essential for optimizing battery performance. Copper (Cu) enhances electrical conductivity and capacity through numerous redox-active sites and maintains high-rate capability without capacity fading. Iron (Fe) is cost-effective and stable, with mixed valence states (Fe^{2+}/Fe^{3+}) enhancing conductivity and capacity, and providing excellent electrochemical stability. Manganese (Mn) increases the efficiency of ion insertion and deinsertion, with large pore structures offering high ion diffusion rates and various oxidation states improving capacity and cycle life. Applied in metal ion batteries, these transition metals collectively enhance the performance of MOF cathodes by improving conductivity, capacity, and stability.

METAL-ORGANIC FRAMEWORK CATHODE CATALYSTS IN METAL-AIR BATTERIES

A metal-air battery possesses both features of a fuel cell and a rechargeable battery that generates electricity through an electrochemical reaction using metal as the anode and oxygen in the air as the cathode. The open cell that utilizes oxygen in air as a reactant differentiates it from other metal-ion batteries.[72] This allows light weight while continuously receiving oxygen from an external source, increasing the miniaturization potential of the battery, and providing high theoretical energy density and price competitiveness. As shown in Figure 6, the overall theoretical gravimetric and volumetric energy densities of metal-air batteries, such as Li-Air, Zn-Air, and Al-air batteries (AABs), are very high. These advantages make it promising for next-generation portable batteries and energy storage systems.[73]

The oxidation-reduction reaction of oxygen in the cathode catalyst depends on the type of electrolyte, and each reaction is thermodynamically reversible. However, in terms of kinetics, electron transport is difficult; therefore, metal-air batteries have a slow reaction rate and high overpotential. Consequently, metal-air batteries have low energy efficiency and many efforts have been made to solve this. Among them,

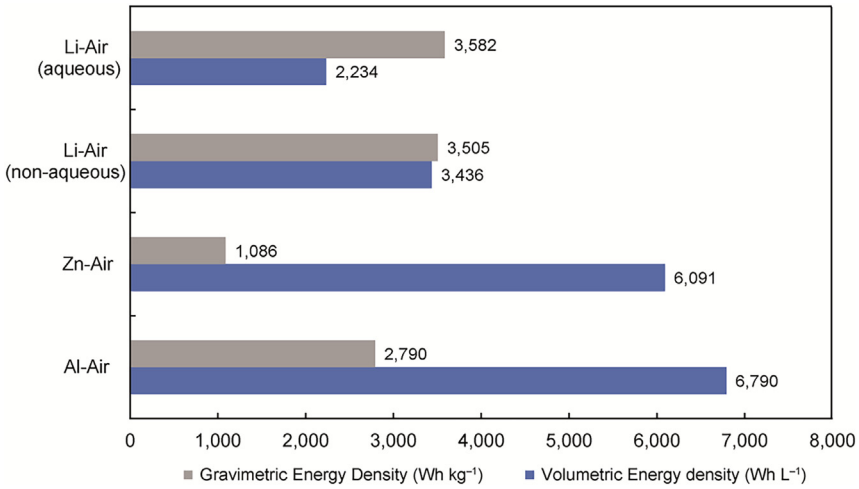

Figure 6. Energy density of metal-air batteries

Theoretical gravimetric and volumetric energy density of metal-air batteries.[75]

improving the performance of the catalyst used in the cathode has the most direct effect. Noble metals and their alloys have been proposed as cathodic catalysts. Precious metals such as Pt, Ru, and Ir have been used, and their alloys (Pt-Ir, etc.), which combine the advantages of each constituent precious metal have also been presented.[74] However, their low durability and high cell manufacturing costs are obstacles to their widespread adoption. Moreover, noble metal catalysts do not bifunctionally catalyze oxygen reduction reactions (ORR) and oxygen evolution reactions (OER).

Non-precious metal-based catalysts have been developed.[75] They reduce the overpotentials generated during the charge-discharge reaction by dual functional catalytic effects on both the ORR and OER. However, these types of catalysts have poor electrical conductivity. Thus, efforts have been made to develop an electrically conductive material capable of catalyzing redox reactions at a competitive price. Recently, various studies have been conducted to improve the battery performance and efficiency by directly introducing MOFs as cathodic catalysts. In this section, we analyze the studies that have produced high-performance cathodic catalysts by directly grafting MOFs to the catalysts according to the type of battery.

Metal-organic framework cathode catalysts in lithium-air batteries

Li-air batteries (LABs) perform a high theoretical gravimetric energy density of approximately 11,700 Wh kg^{-1} and a high volumetric energy density of 2,800 Wh L^{-1}. The LAB reaction proceeds as $2Li^+ + O_2 + 2e^- \rightleftarrows Li_2O_2$ with $E_o = 2.96$ V (vs. Li/Li^+)[76–78] and oxygen can be obtained as fuel through the cathode.[79] However, LABs still have disadvantages, such as low energy efficiency, limited cyclability, and the occurrence of various side reactions due to free radicals produced during the reaction of oxygen.[80]

LABs, like other metal-air batteries, have a slow electrochemical reaction with oxygen and consume a lot of energy; therefore, much research has been conducted on the development of cathode catalysts, such as bimetallic composites with noble metals or transition metal oxides.[81–83] Unfortunately, the mechanism of operation of these catalysts promotes the formation and decomposition of Li_2O_2 discharge products. By-products, such as Li_2O_2, are deposited on the surface and pores of the cathode during the discharge-charge process of the battery, blocking the diffusion paths of Li^+ and O_2. These limitations of LABs can be overcome by replacing the conventional cathode catalysts with MOFs.

The transition metals in MOFs can act as open active sites and provide high O_2 accessibility and catalytic activity with a porous structure (Figure 2B). In particular, the modularity of transition metals and organic linkers in MOF structures provides opportunities to control their electrical conductivity, catalytic activity, surface area, and open active sites of transition metals. Therefore, in this section, MOF cathode catalysts in LABs are classified based on the transition metal center and organic linkers and the performance results of MOF-based cathode modification trials are summarized. Table 1 lists the comprehensive details of LAB MOF cathodes.

First, studies have been conducted to improve the performance of MOF cathodic catalysts by optimizing the transition metals (Figure 2A). Kim et al. synthesized[84] bimetallic MnCo-MOF-74 as a cathode catalyst which has a large number of open transition metal active sites that effectively adsorb O_2. Mn and Co were mixed at a ratio of approximately 1:4 to form a stable hexagonal rod-shaped porous structure resulting in a high discharge capacity (11,150 mAh g^{-1} at a current density of 200 mA g^{-1}) and stable discharge capacity (1,000 mAh g^{-1} for 44 cycles at 200 mA g^{-1}). Yan et al. proposed[85] Co-MOF-74, which can form short diffusion paths providing access to the active O_2 and Li^+ sites while maintaining a high internal surface area. Nanorod and nanofiber structures are possible, resulting in Co-MOF-74-X (X = 1400, 800, or 20 nm, where X denotes the average width of the prepared nanorods and nanofibers). It has been proven that when a regulator and additives are introduced to reduce the size, the diffusion path becomes shorter as the size decreases, and the performance of the battery improves. Reducing the crystal size of the Co-MOF-74-X catalyst enabled a high discharge capacity (11,350 mAh g^{-1} at 100 mA g^{-1} and 6,640 mAh g^{-1} at 500 mA g^{-1}) and good rate performance.

Yuan et al. synthesized[86] 2D Mn-MOF and observed that their 2D structure enabled excellent oxygen evolution and reduction reactions and efficient oxidation between LiOH and Li_2O_2. 2D Mn-MOF has a large specific surface area, abundant open active sites, and a highly electrocatalytically active Mn-O cluster. It enables effective mass transfer and the transport of O_2 and Li^+ and promotes the decomposition of Li_2O_2. It shows a high discharge capacity (9,464 mAh g^{-1} at 1,000 mA g^{-1}), a round-trip efficiency of 68.5%, and a specific capacity of 1000 mAh g^{-1} after 200 cycles at 100 mA g^{-1}.

Hu et al. used[87] Ni-based organic frameworks of Ni(4,4-bipy)(H_3BTC) (4,4-bipy = 4,4-bipyridine; H_3BTC = 1,3,5-benzenetricarboxylic acid) (Ni-MOFs) to fabricate a high-performance cathode catalyst. Ni-MOF has a 3D microstructure, open catalytic sites, and a large surface area to facilitate the transport of O_2 and Li^+. The LAB using the Ni-MOF catalyst showed a high capacity of 9000 mAh g^{-1} at 0.12 mA cm^{-2}, a high coulombic efficiency of 80%, and a respectable cyclability of 170 cycles without any voltage drop.

Wu et al. evaluated[88] MOF-5[$Zn_4O(BDC)_3$, BDC = 1,4-benzenedicarboxylate], HKUST-1[$Cu_3(BTC)_2$, BTC = benzene-1,3,5-tricarboxylate], and M-MOF-74 (M = Mg, Mn, Co) and obtained MOFs with extensive surface areas, various structural topologies, and exclusive metal sites accessibility. It was found that Mn-MOF-74 can achieve 9420 mAh g^{-1} capacity at 50 mA g^{-1} in LABs.

Secondarily, an excellent-performance MOF cathode catalyst was developed by optimizing the organic linker. Li et al. developed[89] a nanoporous MOF, Tz-Mg-MOF-74, using a 1,2,4,5-tetrazine (Tz)-functionalized ligand that exhibits excellent stability in organic solvents and has redox activity. It promotes the formation of stable anion radicals by matching the charge-discharge reaction rate and can adsorb Li^+. These effects prevented the solvation of small molecules and improved the electrochemical performance with the sustainable discharge capacity (7700 mAh g^{-1} at 50 mA g^{-1}) and low overpotential.

Suppressing the formation of the Li_2O_2 by-product, which is the main cause of degradation of LAB performance, and channel formation for smooth Li^+ and O_2 transport are major goals of research on MOF cathode catalysts. One approach involves changing the type of transition metals or organic linkers. Others attempted to solve this problem by using composite structures. For example, Zhang et al. designed[90] MOF-74 (MOF-74@CNTs) grown directly on carbon nanotubes (CNTs) to improve the low electrical conductivity of MOFs. CNTs were used as substrates for the growth of MOF-74 nanoparticles, providing a conductive network and alleviating the aggregation of MOF NPs, allowing them to be used as effective cathode catalysts. In particular, it is a cathodic catalyst that can operate in a humid oxygen atmosphere and enables LAB operation under practical conditions by utilizing a chemical catalytic conversion reaction mechanism that converts Li_2O_2 to LiOH. However, this strategy did not improve the electrical conductivity of the MOF itself.

Metal-organic framework cathode catalysts in zinc-air batteries

Zn-Air batteries (ZABs) are capable of high theoretical gravimetric energy densities of 1,086 Wh kg^{-1} and theoretical volumetric energy densities up to 6,091 Wh L^{-1} (including atmospheric oxygen fuel at the air cathode).[91] In particular, eco-friendliness[92,93] due to the use of aqueous electrolytes and the price competitiveness of raw materials of ZABs are promoting their development. It also has the second highest gravimetric energy density by weight when compared to LABs, while its gravimetric energy density by volume is the highest among other renewable energy sources. However, ZABs are limited by their slow ORR and OER kinetics and high overpotentials.[94] Similar to other air batteries, cathode catalysts using noble metals or metal oxides have been developed for ZABs. However, ZABs face problems such as the significant deterioration in electrical conductivity during operation and their high cost due to insufficient reserves of required materials.[95,96] Therefore, MOFs have been actively proposed as cathode catalysts for ZABs to solve these problems.

First, dimensional tunability resulting from various structural motifs of MOFs as cathode catalysts has been studied. Shinde et al. proposed[97] a novel 3D dual-linked hexaiminobenzene MOF (Mn/Fe-HIB-MOF) (electrical conductivity of 359 S cm^{-1}.[22]) as a material that can provide a high surface area and porosity. This MOF used hexaiminobenzene as an organic linker to act as a bifunctional oxygen electrocatalyst with high crystallinity, electrical conductivity, and chemical compatibility. It was introduced into quintet-shelled hollow spheres with a precisely controlled M^{2+} (M = Mn, Fe) species. A high surface area (2298 m^2 g^{-1}), 1000 h (at 10 mA cm^{-2} with trivial voltage fading) cycle life, high energy density (1027 Wh kg^{-1}), and a small discharging-charging voltage gap were achieved.

Second, the electrochemical activity can be increased by utilizing the hierarchical structure of MOFs. The unique hierarchical structure of MOFs boosts electrocatalytic activity by offering porous channels and exposing the active open metal sites. Weixin Li. et al. designed[98] a hybrid Co-and Fe-based metal-organic framework (HCF-MOF) as a bifunctional catalyst capable of performing both oxygen redox reactions. A unique MOF hierarchical structure composed of subunits of nanosheets and nanoparticles can be created by changing the molar ratio of Co to Fe. This approach resulted in the formation of porous channels capable of electron and mass transport and improved the exposure of the transition metal active sites. This demonstrates a modest OER overpotential of 295 mV at 10 mA cm^{-2} with a small Tafel slope of 42 mV dec^{-1} and high-power density of 113.5 mW cm^{-2}.

All the aforementioned studies utilized the structural characteristics of MOFs to apply MOFs as cathode catalysts for ZABs. Other studies have been conducted on composites by combining materials that can offset the shortcomings of MOFs.[99] There are lots of efforts to apply the MOF to function as a cathode catalyst. Although the MOF composites strategy is also a good way to commercialize the MOF cathode catalyst in zinc-air batteries, additional research is needed to maximize the performance of the MOF itself.

Metal-organic framework cathode catalysts in aluminum-air batteries

AABs show a high theoretical capacity of 2980 mAh g^{-1}, a high theoretical voltage of 2.7 V, and an energy density of 8100 Wh kg^{-1}. In addition, because Al is abundant and highly recyclable, it has many economic advantages and AABs have great potential as a next-generation battery system. The AAB cathode is commonly composed of a catalytic active layer, a gas diffusion layer, and a current collector. This composite

cathode structure is a half-open system, which is a characteristic of the metal-air battery.[100–103] However, as with both the LAB and ZAB systems discussed earlier, the ORR occurring at the cathode is very slow and determines the overall reaction rate. These sluggish ORR reactions reduce energy efficiency and cause high overpotentials in the AAB system. Therefore, to increase the ORR rate, an effective catalytically active layer containing a new type of electrocatalyst capable of lowering the activation energy is essential. Therefore, it is necessary to fabricate cathode catalysts that can efficiently react with oxygen and have good durability.

Typical catalysts include noble metals and alloys (Pt, Pd, Au, Ag, etc.), transition metal oxides/chalcogenides, metal macrocyclic compounds, and carbonaceous materials.[104] However, they cause aluminum self-corrosion during discharge and open-circuit conditions in alkaline solutions. In addition, at the anode side, the accumulation of by-products, such as Al_2O_3 and $Al(OH)_3$, blocks the oxygen inflow path and inhibits diffusion. Accordingly, there has been a recent trend to use MOFs as cathode catalysts to solve these problems. Therefore, in this section, we analyze various studies that directly utilize MOFs as cathode catalysts and present directions for their future development.

Mori et al. reported the only study[105] that uses the MOF itself as a cathode catalyst for AABs. Aluminum terephthalate (AT) was used as the active material for the cathode catalytic layer and a battery with the ionic-liquid electrolyte 1-ethyl-3-methylimidazolium chloride was constructed. Although it had a lower electrical power output and cell capacity than activated carbon, stable cycling was possible. This was expected because the formation of $Al(OH)_3$ and Al_2O, which are major by-products of AAB, was suppressed, and the interfacial resistance of the cell did not significantly increase after several cycles. However, research on new MOFs that can improve not only stability, but also electrochemical performance must be continued.

METAL-ORGANIC FRAMEWORK CATHODES IN LITHIUM-SULFUR BATTERIES

The development of advanced batteries for grid storage, EVs, and portable devices must have cost-effectivity and high energy density. LSBs have been proposed as next-generation battery candidates that can meet these requirements.[106,107] The use of sulfur, which is abundant in nature and has a high gravimetric energy density (2567 Wh kg^{-1}), significantly reduces the battery production cost. Consequently, a sulfur-based battery with high specific capacity (1675 mAh g^{-1}) can be realized.[76] However, LSBs exhibit poor cycling performance due to insufficient reversibility of the cleavage/formation reactions of stable sulfur molecules (S_8).[108] Additionally, the "shuttle effect" and volume expansion caused by the dissolution of the polysulfide species (Li_2S_8, Li_2S_6, Li_2S_4, and Li_2S_3) during the electrochemical reaction cause rapid capacity decay and low coulombic efficiency.[109,110]

To solve the abovementioned issues, strategies for fixing sulfur using porous material scaffolds have been reported.[111–115] Sulfur-encapsulating porous materials include carbonaceous materials,[116,117] conductive polymers,[118,119] and transition metal oxides.[120–122] MOFs are also attractive materials that can play this role, and research on fixing sulfur using a frame consisting of metal ions and organic linkers has been actively conducted.[123] MOFs have a higher crystallinity than other porous materials and the electrically conductive properties of the chemically active sites in the scaffold such as the functional groups of the transition metals and the organic linkers can be utilized. Therefore, it is necessary to develop a stable MOF that can trap sulfur and polysulfide species while maintaining its permanently porous structure (Figure 7A). Many studies have been conducted to develop methods for improving the performance of LSBs by utilizing these optimized MOFs. As shown in Figure 7, the MOF cathodes can encapsulate sulfur (S) in their pore structures (Figure 7A), and the organic linker (Figure 7B) of the MOF can react with Li^+ ions by increasing the number of redox-active sites. The high porosity and large surface area of MOFs facilitate the efficient confinement of sulfur, mitigating the shuttle effect by physically trapping polysulfides within the framework. Additionally, the tunable pore size of MOFs allows for the optimization of ion transport pathways, enhancing the overall electrochemical performance. Furthermore, the presence of metal nodes and organic linkers in MOFs contributes to the catalytic conversion of polysulfides, further improving the cycling stability and capacity retention of the batteries. In this section, the MOFs used in LSBs are discussed and analyzed to help direct future research on the development of high-performance MOF cathodes for LIBs. In this section, the MOFs used in LSBs are discussed and analyzed to help direct future research on the development of high-performance MOF cathodes for LIBs. Table 1 outlines the overall capacities of MOF cathodes focusing on LSB.

First, the MOFs for LSBs must be stiff so that sulfur can be confined. Hong et al. constructed[124] a cage-like MOF, Cu-TDPAT, using 2,4,6-tris-(3,5-dicarboxylphenyl-amino)-1,3,5-triazine (H_6TDPAT) as the ligand. It has abundant open metal (Cu(II)) and nitrogen functional sites, which are mainly used as hosts in LSBs. Thus, S atoms can be sufficiently confined, and the MOF size can be optimized to the nanoscale. The resulting LSB exhibited a reversible capacity of 745 mAh g^{-1} at 1675 mA g^{-1} after 500 cycles and achieved a better performance than previously reported S@MOF materials. Feng et al. synthesized[125] Cu-MOF using benzene-1,3,5-tricarboxylic acid as the ligand. This Cu-MOF can function as a sulfur-confinement host for LSBs, and the pore size can also be adjusted. In this study, the Cu-MOF exhibited a specific capacity of 1051.3 mAh g^{-1} after 300 cycles at a charge/discharge current density of 200 mA g^{-1}. In addition, the Cu-MOF had a high sulfur content of 19.3 wt % or more, while effectively suppressing the capacity reduction and improving the coulombic efficiency. Wang et al. also synthesized[126] MOF-525(Cu) MOFs with a unique structure. In this study, the Cu^{2+} sites of MOF-525(Cu) provided two Lewis acidic sites, which acted as powerful MOF hosts for the inclusion of sulfur and polysulfides. MOF-525(Cu) provided the appropriate reaction environment for sulfur and polysulfide. Also, the MOF-525(Cu) permanent porous structure resulted in good electrochemical stability during cycling and the battery produced 700 mAh g^{-1} at approximately 325 mA g^{-1} after 200 cycles. Zeng et al. synthesized[127] MOF-TOC by incorporating Ti-O clusters (TOCs) within the mesopore of MIL-101. Therefore, sulfur can be effectively stored in the pores of MIL-101, and TOCs facilitate the conversion of lithium polysulfide through d-p orbital hybridization between Ti and sulfur. This highly catalytic sulfur host provided a capacity of 964 mAh g^{-1} at 1675 mA g^{-1} and showed good capacity retention of 83.5% after 500 cycles.

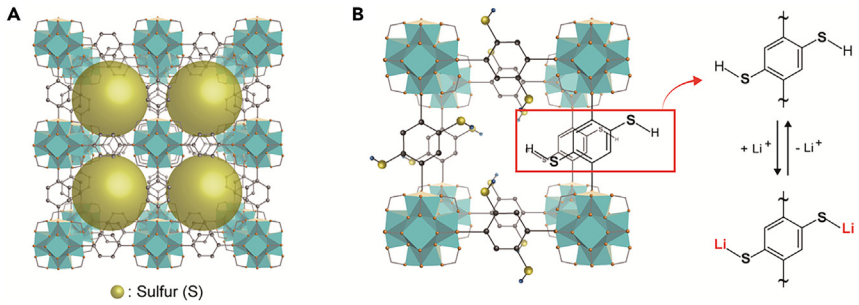

Figure 7. Strategies for using MOFs for sulfur cathodes

(A) Sulfur(S) encapsulation by the pore structure of MOF (yellow spheres can confine S).

(B) Redox reaction between the organic linker of MOF and the lithium ion.[127–129]

Second, MOFs for LSB cathodes can inhibit the dissolution of sulfur species in the electrolyte. Shimizu et al. synthesized[128] disulfide-ligand-containing MOFs (DS-MOFs) with various dimensions. The structure contains various disulfide ligands with flexible S-S bonds that can reversibly perform S-S cleavage and formation. The porous structure of the MOFs in the LSB cathode allows Li^+ ions to easily access the redox-active sites, thus maximizing the capacity utilization of the cathode material. Moreover, the cycling performance can be improved by changing the structural dimensions of the MOFs. It was determined that the robust crystalline structure of the MOF played a role in preventing the dissolution of S species. Liu et al. proposed[129] a strategy for covalently binding porous MOFs with sulfur. In this study, CNT@UIO-66-SH (electrical conductivity of 10^{-5} to 10^{-7} S cm^{-1}.[130]) was synthesized, which forms a covalent bond with sulfur to stabilize sulfur and physically absorbs polysulfide species during battery cycling. This allowed a discharge capacity of 608 mAh g^{-1} at a rate of 1675 mA g^{-1} after 450 cycles and a small decay of 0.017% per cycle.[131] In addition, strategies have been developed to fabricate composites by hybridizing MOF and CNTs[132] or to fabricate LSB cathodes using materials derived from MOF.[133] However, since the improvement of the conductivity of the MOF cathode through the introduction of CNTs lowers the energy density, research in the direction of increasing the conductivity of the MOF itself, like the conductive MOF, is more desirable. In Figure 8, a comparison is made between the mean voltage and capacity of MOF cathodes and those of typical cathodes used in LSBs.

CONCLUSION AND OUTLOOK

In this review, batteries using MOFs as cathode materials or composite cathode materials were organized according to the battery type (Table 1). MOFs with the desired porosity, crystallinity, and chemical/mechanical properties can be fabricated by selecting the appropriate combinations of transition metals and organic linkers. These MOF characteristics show great promise for the development of MOF cathodes. We classified MOF cathodes into three major applications: metal-ion batteries, metal-air batteries, and Li-S batteries. Thereafter, the features of the MOFs required by the cathode of each battery system were analyzed. The studies summarized in this review demonstrate that the direct

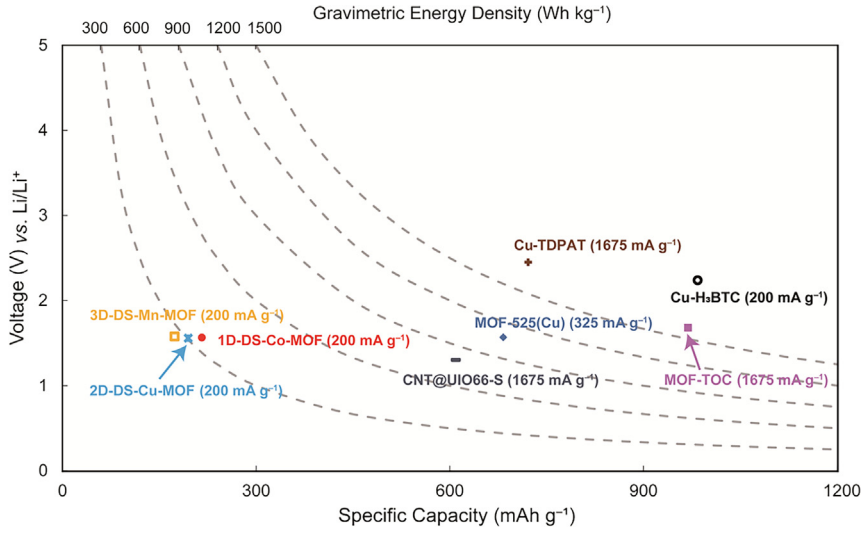

Figure 8. Operation voltage versus specific capacities of lithium-sulfur battery electrode materials

Comparison of performance between various MOF cathodes and representative commercial cathode materials in LSBs.[124–129]

application of MOFs to cathodes or cathode composites enables the fabrication of a variety of battery systems with superior electrochemical performance and capacity.

However, continuous researches are still required to enable MOFs to be fully applied as active materials for cathodes. First, it is necessary to clearly determine the behavior of ions and electrons inside MOFs to develop MOFs with very high electrical and ionic conductivities. Hybridizing an electronically conductive material with the MOF can improve the conductivity but reduce the energy density; thus, it is necessary to increase the conductivity of the MOF itself. In addition, the porous structure of the MOFs should be permanently preserved so that the intercalation/deintercalation of metal ions can be reversibly performed during the charge-discharge process. Although the transition metal acts as an open metal site in MOFs and increases the energy capacity because of its role as a redox-active center, it also participates in the reaction and causes dissolution, which eventually collapses the structure. To suppress this, it is important to develop MOFs with higher crystallinity and electrochemical stability. Also, by adjusting structural properties such as strengthening electronic distribution using mixed valence characteristics of metal ions or introducing additional electroactive sites, the low conductivity of MOF cathode can be enhanced.

Finally, for the commercialization of MOF cathodes, it is necessary to simplify the manufacturing process and increase their yield. Therefore, a low-cost, high-efficiency MOF synthesis process must be developed. This review presents the current state of MOF research, the strategies used to develop MOFs with high electrochemical performance and stability, as well as the challenges that still need to be overcome to enable the widespread adoption of MOF cathode batteries. Considering the infinite development potential of MOFs, efforts must be redoubled to solve these remaining challenges.

ACKNOWLEDGMENTS

K.W.N. acknowledges support from the National Research Foundation of Korea through the Excellent Young Scientist Program (NRF-2022R1C1C1007133). This research was supported by the BK21 FOUR (Fostering Outstanding Universities for Research) funded by the Ministry of Education (MOE, Korea) and NRF (NRF-5199990614253, Education Research Center for 41R-Based Health Care).

AUTHOR CONTRIBUTIONS

K.W.N. proposed the outline and guided the manuscript. J.L., I.C., J.P., and E.K. organized the manuscript. All authors contributed to the discussion and completion of the manuscript.

DECLARATION OF INTERESTS

The authors declare no competing interests.

REFERENCES

1. Dresselhaus, M.S., and Thomas, I.L. (2001). Alternative energy technologies. Nature *414*, 332–337. https://doi.org/10.1038/35104599.
2. Williams, J.H., DeBenedictis, A., Ghanadan, R., Mahone, A., Moore, J., Morrow, W.R., 3rd, Price, S., and Torn, M.S. (2012). The technology path to deep greenhouse gas emissions cuts by 2050: the pivotal role of electricity. Science *335*, 53–59. https://doi.org/10.1126/science.1208365.
3. Armand, M., and Tarascon, J.-M. (2008). Building better batteries. Nature *451*, 652–657. https://doi.org/10.1038/451652a.
4. Dunn, B., Kamath, H., and Tarascon, J.-M. (2011). Electrical energy storage for the grid: a battery of choices. Science *334*, 928–935. https://doi.org/10.1126/science.1212741.
5. Aricò, A.S., Bruce, P., Scrosati, B., Tarascon, J.-M., and Van Schalkwijk, W. (2005). Nanostructured materials for advanced energy conversion and storage devices. Nat. Mater. *4*, 366–377. https://doi.org/10.1038/nmat1368.
6. Goodenough, J.B., and Park, K.-S. (2013). The Li-ion rechargeable battery: a perspective. J. Am. Chem. Soc. *135*, 1167–1176. https://doi.org/10.1021/ja3091438.
7. Lin, R., Hu, E., Liu, M., Wang, Y., Cheng, H., Wu, J., Zheng, J.-C., Wu, Q., Bak, S., Tong, X., et al. (2019). Anomalous metal segregation in lithium-rich material provides design rules for stable cathode in lithium-ion battery. Nat. Commun. *10*, 1650. https://doi.org/10.1038/s41467-019-09248-0.
8. Ji, H., Wu, J., Cai, Z., Liu, J., Kwon, D.-H., Kim, H., Urban, A., Papp, J.K., Foley, E., Tian, Y., et al. (2020). Ultrahigh power and energy density in partially ordered lithium-ion cathode materials. Nat. Energy *5*, 213–221. https://doi.org/10.1038/s41560-020-0573-1.
9. Xu, J., Lin, F., Doeff, M.M., and Tong, W. (2017). A review of Ni-based layered oxides for rechargeable Li-ion batteries. J. Mater. Chem. A *5*, 874–901. https://doi.org/10.1039/C6TA07991A.
10. Li, W., Erickson, E.M., and Manthiram, A. (2020). High-nickel layered oxide cathodes for lithium-based automotive batteries. Nat. Energy *5*, 26–34. https://doi.org/10.1038/s41560-019-0513-0.
11. Whittingham, M.S. (1976). Electrical energy storage and intercalation chemistry. Science *192*, 1126–1127. https://doi.org/10.1126/science.192.4244.1126.
12. Li, H., Eddaoudi, M., O'Keeffe, M., and Yaghi, O.M. (1999). Design and synthesis of an exceptionally stable and highly porous metal-organic framework. Nature *402*, 276–279. https://doi.org/10.1038/46248.
13. Zhou, H.-C., Long, J.R., and Yaghi, O.M. (2012). Introduction to metal–organic frameworks. Chem. Rev. *112*, 673–674. https://doi.org/10.1021/cr300014x.
14. Furukawa, H., Cordova, K.E., O'Keeffe, M., and Yaghi, O.M. (2013). The chemistry and applications of metal-organic frameworks. Science *341*, 1230444. https://doi.org/10.1126/science.1230444.
15. Li, S.-L., and Xu, Q. (2013). Metal–organic frameworks as platforms for clean energy. Energy Environ. Sci. *6*, 1656–1683. https://doi.org/10.1039/C3EE40507A.
16. Lu, C., Clayville, B., Choi, J.Y., and Park, J. (2023). 2D metal-organic frameworks as an emerging platform with tunable electronic structures. Chem *9*, 2757–2770. https://doi.org/10.1016/j.chempr.2023.06.005.
17. Sheberla, D., Bachman, J.C., Elias, J.S., Sun, C.-J., Shao-Horn, Y., and Dincă, M. (2017). Conductive MOF electrodes for stable supercapacitors with high areal capacitance. Nat. Mater. *16*, 220–224. https://doi.org/10.1038/nmat4766.
18. Feng, D., Lei, T., Lukatskaya, M.R., Park, J., Huang, Z., Lee, M., Shaw, L., Chen, S., Yakovenko, A.A., Kulkarni, A., et al. (2018). Robust and conductive two-dimensional metal− organic frameworks with exceptionally high volumetric and areal capacitance. Nat. Energy *3*, 30–36. https://doi.org/10.1038/s41560-017-0044-5.
19. Sun, L., Campbell, M.G., and Dincă, M. (2016). Electrically conductive porous metal–organic frameworks. Angew. Chem. Int. Ed. Engl. *55*, 3566–3579. https://doi.org/10.1002/anie.201506219.
20. Bai, S., Kim, B., Kim, C., Tamwattana, O., Park, H., Kim, J., Lee, D., and Kang, K. (2021). Permselective metal–organic framework gel membrane enables long-life cycling of rechargeable organic batteries. Nat.

Nanotechnol. *16*, 77–84. https://doi.org/10.1038/s41565-020-00788-x.

21. Wang, Q., and Astruc, D. (2020). State of the art and prospects in metal–organic framework (MOF)-based and MOF-derived nanocatalysis. Chem. Rev. *120*, 1438–1511. https://doi.org/10.1021/acs.chemrev.9b00223.
22. Xie, L.S., Skorupskii, G., and Dincă, M. (2020). Electrically conductive metal–organic frameworks. Chem. Rev. *120*, 8536–8580. https://doi.org/10.1021/acs.chemrev.9b00766.
23. Zhou, Y.-N., Ma, J., Hu, E., Yu, X., Gu, L., Nam, K.-W., Chen, L., Wang, Z., and Yang, X.-Q. (2014). Tuning charge–discharge induced unit cell breathing in layer-structured cathode materials for lithium-ion batteries. Nat. Commun. *5*, 5381. https://doi.org/10.1038/ncomms6381.
24. Sun, Y., Lee, H.-W., Seh, Z.W., Liu, N., Sun, J., Li, Y., and Cui, Y. (2016). High-capacity battery cathode prelithiation to offset initial lithium loss. Nat. Energy *1*, 1–7. https://doi.org/10.1038/nenergy.2015.8.
25. Lin, F., Nordlund, D., Li, Y., Quan, M.K., Cheng, L., Weng, T.-C., Liu, Y., Xin, H.L., and Doeff, M.M. (2016). Metal segregation in hierarchically structured cathode materials for high-energy lithium batteries. Nat. Energy *1*, 1–8. https://doi.org/10.1038/nenergy.2015.4.
26. Ohzuku, T., Ueda, A., and Nagayama, M. (1993). Electrochemistry and structural chemistry of LiNiO2 (R3m) for 4 volt secondary lithium cells. J. Electrochem. Soc. *140*, 1862–1870. https://doi.org/10.1149/1.2220730.
27. Lin, F., Markus, I.M., Nordlund, D., Weng, T.-C., Asta, M.D., Xin, H.L., and Doeff, M.M. (2014). Surface reconstruction and chemical evolution of stoichiometric layered cathode materials for lithium-ion batteries. Nat. Commun. *5*, 3529. https://doi.org/10.1038/ncomms4529.
28. Lung-Hao Hu, B., Wu, F.-Y., Lin, C.-T., Khlobystov, A.N., and Li, L.-J. (2013). Graphene-modified LiFePO4 cathode for lithium ion battery beyond theoretical capacity. Nat. Commun. *4*, 1687. https://doi.org/10.1038/ncomms2705.
29. Luo, K., Roberts, M.R., Hao, R., Guerrini, N., Pickup, D.M., Liu, Y.-S., Edström, K., Guo, J., Chadwick, A.V., Duda, L.C., and Bruce, P.G. (2016). Charge-compensation in 3 d-transition-metal-oxide intercalation cathodes through the generation of localized electron holes on oxygen. Nat. Chem. *8*, 684–691. https://doi.org/10.1038/nchem.2471.
30. Yan, P., Zheng, J., Liu, J., Wang, B., Cheng, X., Zhang, Y., Sun, X., Wang, C., and Zhang, J.-G. (2018). Tailoring grain boundary structures and chemistry of Ni-rich layered cathodes for enhanced cycle stability of lithium-ion batteries. Nat. Energy *3*, 600–605. https://doi.org/10.1038/s41560-018-0191-3.
31. Radin, M.D., Vinckeviciute, J., Seshadri, R., and Van der Ven, A. (2019). Manganese oxidation as the origin of the anomalous capacity of Mn-containing Li-excess cathode materials. Nat. Energy *4*, 639–646. https://doi.org/10.1038/s41560-019-0439-6.
32. Park, K., Yu, B.-C., Jung, J.-W., Li, Y., Zhou, W., Gao, H., Son, S., and Goodenough, J.B. (2016). Electrochemical nature of the cathode interface for a solid-state lithium-ion battery: interface between $LiCoO_2$ and garnet-$Li_7La_3Zr_2O_{12}$. Chem. Mater. *28*, 8051–8059. https://doi.org/10.1021/acs.chemmater.6b03870.
33. Chen, Q., Xiao, P., Pei, Y., Song, Y., Xu, C.-Y., Zhen, L., and Henkelman, G. (2017). Structural transformations in Li_2MnSiO_4: evidence that a Li intercalation material can reversibly cycle through a disordered phase. J. Mater. Chem. A *5*, 16722–16731. https://doi.org/10.1039/C7TA03049E.
34. Xu, G.-L., Liu, Q., Lau, K.K.S., Liu, Y., Liu, X., Gao, H., Zhou, X., Zhuang, M., Ren, Y., Li, J., et al. (2019). Building ultraconformal protective layers on both secondary and primary particles of layered lithium transition metal oxide cathodes. Nat. Energy *4*, 484–494. https://doi.org/10.1038/s41560-019-0387-1.
35. Stavila, V., Talin, A.A., and Allendorf, M.D. (2014). MOF-based electronic and opto-electronic devices. Chem. Soc. Rev. *43*, 5994–6010. https://doi.org/10.1039/C4CS00096J.
36. Tu, B., Pang, Q., Xu, H., Li, X., Wang, Y., Ma, Z., Weng, L., and Li, Q. (2017). Reversible redox activity in multicomponent metal–organic frameworks constructed from trinuclear copper pyrazolate building blocks. J. Am. Chem. Soc. *139*, 7998–8007. https://doi.org/10.1021/jacs.7b03578.
37. Rosen, A.S., Mian, M.R., Islamoglu, T., Chen, H., Farha, O.K., Notestein, J.M., and Snurr, R.Q. (2020). Tuning the redox activity of metal–organic frameworks for enhanced, selective O_2 binding: Design rules and ambient temperature O_2 chemisorption in a cobalt–triazolate framework. J. Am. Chem. Soc. *142*, 4317–4328. https://doi.org/10.1021/jacs.9b12401.
38. Goodenough, J.B., and Kim, Y. (2010). Challenges for rechargeable Li batteries. Chem. Mater. *22*, 587–603. https://doi.org/10.1021/cm901452z.
39. Sun, Y., Liu, N., and Cui, Y. (2016). Promises and challenges of nanomaterials for lithium-based rechargeable batteries. Nat. Energy *1*, 1–12. https://doi.org/10.1038/nenergy.2016.71.
40. Guan, S., Li, J., Wang, Y., Yang, Y., Zhu, X., Ye, D., Chen, R., and Liao, Q. (2023). Multifunctional MOF-derived Au, Co-doped porous Carbon Electrode for Wearable Sweat Energy Harvesting-storage Hybrid System. Adv. Mater. *35*, e2304465. https://doi.org/10.1002/adma.202304465.
41. Jiang, M., Su, J., Song, X., Zhang, P., Zhu, M., Qin, L., Tie, Z., Zuo, J.-L., and Jin, Z. (2022). Interfacial reduction nucleation of noble metal nanodots on redox-active metal–organic frameworks for high-efficiency electrocatalytic conversion of nitrate to ammonia. Nano Lett. *22*, 2529–2537. https://doi.org/10.1021/acs.nanolett.2c00446.
42. Dong, A., Chen, D., Li, Q., and Qian, J. (2023). Metal-Organic Frameworks for Greenhouse Gas Applications. Small *19*, 2201550. https://doi.org/10.1002/smll.202201550.
43. Skorupskii, G., Trump, B.A., Kasel, T.W., Brown, C.M., Hendon, C.H., and Dincă, M. (2020). Efficient and tunable one-dimensional charge transport in layered lanthanide metal–organic frameworks. Nat. Chem. *12*, 131–136. https://doi.org/10.1038/s41557-019-0372-0.
44. Jiang, Q., Xiong, P., Liu, J., Xie, Z., Wang, Q., Yang, X.Q., Hu, E., Cao, Y., Sun, J., Xu, Y., and Chen, L. (2020). A redox-active 2D metal–organic framework for efficient lithium storage with extraordinary high capacity. Angew. Chem. Int. Ed. *59*, 5273–5277. https://doi.org/10.1002/anie.201914395.
45. Jiang, Q., Xiong, P., Liu, J., Xie, Z., Wang, Q., Yang, X.Q., Hu, E., Cao, Y., Sun, J., Xu, Y., et al. (2020). A redox-active 2D metal-organic framework for efficient lithium storage with extraordinary high capacity. Angew. Chem. Int. Ed. Engl. *59*, 5273–5277. https://doi.org/10.1002/anie.201914395.
46. Cai, T., Hu, Z., Gao, Y., Li, G., and Song, Z. (2022). A Rationally Designed Iron–Dihydroxybenzoquinone Metal–Organic Framework as Practical Cathode Material for Rechargeable Batteries. Energy Storage Mater. *50*, 426–434. https://doi.org/10.1016/j.ensm.2022.05.040.
47. Peng, Z., Yi, X., Liu, Z., Shang, J., and Wang, D. (2016). Triphenylamine-based metal–organic frameworks as cathode materials in lithium-ion batteries with coexistence of redox active sites, high working voltage, and high rate stability. ACS Appl. Mater. Interfaces *8*, 14578–14585. https://doi.org/10.1021/acsami.6b03418.
48. Zhang, Z., Yoshikawa, H., and Awaga, K. (2014). Monitoring the solid-state electrochemistry of Cu (2, 7-AQDC)(AQDC= anthraquinone dicarboxylate) in a lithium battery: coexistence of metal and ligand redox activities in a metal–organic framework. J. Am. Chem. Soc. *136*, 16112–16115. https://doi.org/10.1021/ja508197w.
49. Yamada, T., Shiraishi, K., Kitagawa, H., and Kimizuka, N. (2017). Applicability of MIL-101 (Fe) as a cathode of lithium ion batteries. Chem. Commun. *53*, 8215–8218. https://doi.org/10.1039/C7CC01712J.
50. Li, C., Zhang, C., Xie, J., Wang, K., Li, J., and Zhang, Q. (2021). Ferrocene-based metal-organic framework as a promising cathode in lithium-ion battery. Chem. Eng. J. *404*, 126463. https://doi.org/10.1016/j.cej.2020.126463.
51. Geng, J., Ni, Y., Zhu, Z., Wu, Q., Gao, S., Hua, W., Indris, S., Chen, J., and Li, F. (2023). Reversible Metal and Ligand Redox Chemistry in Two-Dimensional Iron–Organic Framework for Sustainable Lithium-Ion Batteries. J. Am. Chem. Soc. *145*, 1564–1571. https://doi.org/10.1021/jacs.2c08273.
52. Zhang, Z., Yoshikawa, H., and Awaga, K. (2016). Discovery of a "bipolar charging" mechanism in the solid-state electrochemical process of a flexible metal–organic framework. Chem. Mater. *28*, 1298–1303. https://doi.org/10.1021/acs.chemmater.5b04075.
53. Férey, G., Millange, F., Morcrette, M., Serre, C., Doublet, M.L., Grenèche, J.M., and Tarascon, J.M. (2007). Mixed-valence Li/Fe-based metal–organic frameworks with both reversible redox and sorption properties. Angew. Chem. Int. Ed. Engl. *46*, 3259–3263. https://doi.org/10.1002/anie.200605163.
54. Nagatomi, H., Yanai, N., Yamada, T., Shiraishi, K., and Kimizuka, N. (2018). Synthesis and electric properties of a two-dimensional metal-organic framework based on phthalocyanine. Chem. Eur J. *24*, 1806–1810. https://doi.org/10.1002/chem.201705530.
55. Du, Z.-Q., Li, Y.-P., Wang, X.-X., Wang, J., and Zhai, Q.-G. (2019). Enhanced electrochemical performance of Li–Co-BTC ternary metal–organic frameworks as cathode materials for lithium-ion batteries.

Dalton Trans. *48*, 2013–2018. https://doi.org/10.1039/C8DT04863K.

56. Kundu, D., Adams, B.D., Duffort, V., Vajargah, S.H., and Nazar, L.F. (2016). A high-capacity and long-life aqueous rechargeable zinc battery using a metal oxide intercalation cathode. Nat. Energy *1*, 1–8. https://doi.org/10.1038/nenergy.2016.119.
57. Ma, L., Schroeder, M.A., Borodin, O., Pollard, T.P., Ding, M.S., Wang, C., and Xu, K. (2020). Realizing high zinc reversibility in rechargeable batteries. Nat. Energy *5*, 743–749. https://doi.org/10.1038/s41560-020-0674-x.
58. Pan, H., Shao, Y., Yan, P., Cheng, Y., Han, K.S., Nie, Z., Wang, C., Yang, J., Li, X., Bhattacharya, P., et al. (2016). Reversible aqueous zinc/manganese oxide energy storage from conversion reactions. Nat. Energy *1*, 1–7. https://doi.org/10.1038/nenergy.2016.39.
59. Zhang, N., Cheng, F., Liu, J., Wang, L., Long, X., Liu, X., Li, F., and Chen, J. (2017). Rechargeable aqueous zinc-manganese dioxide batteries with high energy and power densities. Nat. Commun. *8*, 405. https://doi.org/10.1038/s41467-017-00467-x.
60. Huang, J., Zeng, J., Zhu, K., Zhang, R., and Liu, J. (2020). High-Performance Aqueous Zinc–Manganese Battery with Reversible Mn^{2+}/Mn^{4+} Double Redox Achieved by Carbon Coated MnO_x Nanoparticles. Nano-Micro Lett. *12*, 1–12. https://doi.org/10.1007/s40820-020-00445-x.
61. Wan, F., Zhang, L., Dai, X., Wang, X., Niu, Z., and Chen, J. (2018). Aqueous rechargeable zinc/sodium vanadate batteries with enhanced performance from simultaneous insertion of dual carriers. Nat. Commun. *9*, 1656. https://doi.org/10.1038/s41467-018-04060-8.
62. Zhao, Q., Huang, W., Luo, Z., Liu, L., Lu, Y., Li, Y., Li, L., Hu, J., Ma, H., and Chen, J. (2018). High-capacity aqueous zinc batteries using sustainable quinone electrodes. Sci. Adv. *4*, eaao1761. https://doi.org/10.1126/sciadv.aao1761.
63. Nam, K.W., Park, S.S., Dos Reis, R., Dravid, V.P., Kim, H., Mirkin, C.A., and Stoddart, J.F. (2019). Conductive 2D metal-organic framework for high-performance cathodes in aqueous rechargeable zinc batteries. Nat. Commun. *10*, 4948. https://doi.org/10.1038/s41467-019-12857-4.
64. Wang, Y., Song, J., and Wong, W.Y. (2023). Constructing 2D Sandwich-like MOF/MXene Heterostructures for Durable and Fast Aqueous Zinc-Ion Batteries. Angew. Chem. Int. Ed. Engl. *62*, e202218343. https://doi.org/10.1002/anie.202218343.
65. Ru, Y., Zheng, S., Xue, H., and Pang, H. (2021). Layered V-MOF nanorods for rechargeable aqueous zinc-ion batteries. Mater. Today Chem. *21*, 100513. https://doi.org/10.1016/j.mtchem.2021.100513.
66. Wang, Y., Cao, S., Zhao, J., Zhang, X., Du, X., Li, J., and Wu, F. (2023). Conductive vanadium-based metal-organic framework nanosheets membranes as polysulfide inhibitors for lithium-sulfur batteries. J. Alloys Compd. *960*, 170922. https://doi.org/10.1016/j.jallcom.2023.170922.
67. Mondal, S., Samanta, P., Sahoo, R., Kuila, T., and Das, M.C. (2023). Porous and chemically robust MIL-100 (V) MOF as an efficient cathode material for zinc-ion batteries. Chem. Eng. J. *470*, 144340. https://doi.org/10.1016/j.cej.2023.144340.
68. Pu, X., Jiang, B., Wang, X., Liu, W., Dong, L., Kang, F., and Xu, C. (2020). High-performance aqueous zinc-ion batteries realized by MOF materials. Nano-Micro Lett. *12*, 1–15. https://doi.org/10.1007/s40820-020-00487-1.
69. Kesavan, M., Sannasi, V., Kathiresan, M., and Ramesh, M. (2023). Metal-organic framework (Mn-BTC MOF) incorporated polymer gel electrolytes for dye-sensitized solar cells: preparation and device performances. Bull. Mater. Sci. *46*, 90. https://doi.org/10.1007/s12034-023-02924-4.
70. Yin, C., Pan, C., Liao, X., Pan, Y., and Yuan, L. (2021). Coordinately unsaturated manganese-based metal–organic frameworks as a high-performance cathode for aqueous zinc-ion batteries. ACS Appl. Mater. Interfaces *13*, 35837–35847. https://doi.org/10.1021/acsami.1c10063.
71. Sang, Z., Liu, J., Zhang, X., Yin, L., Hou, F., and Liang, J. (2023). One-Dimensional π–d Conjugated Conductive Metal–Organic Framework with Dual Redox-Active Sites for High-Capacity and Durable Cathodes for Aqueous Zinc Batteries. ACS Nano *17*, 3077–3087. https://doi.org/10.1021/acsnano.2c11974.
72. Lee, J.S., Tai Kim, S., Cao, R., Choi, N.S., Liu, M., Lee, K.T., and Cho, J. (2011). Metal–air batteries with high energy density: Li–air versus Zn–air. Adv. Energy Mater. *1*, 34–50. https://doi.org/10.1002/aenm.201000010.
73. Rahman, M.A., Wang, X., and Wen, C. (2013). High energy density metal-air batteries: a review. J. Electrochem. Soc. *160*, A1759–A1771. https://doi.org/10.1149/2.062310jes.
74. Fan, Z., and Zhang, H. (2016). Template synthesis of noble metal nanocrystals with unusual crystal structures and their catalytic applications. Acc. Chem. Res. *49*, 2841–2850. https://doi.org/10.1021/acs.accounts.6b00527.
75. Han, C., Li, W., Liu, H.-K., Dou, S., and Wang, J. (2019). Design strategies for developing non-precious metal based bi-functional catalysts for alkaline electrolyte based zinc–air batteries. Mater. Horiz. *6*, 1812–1827. https://doi.org/10.1039/C9MH00502A.
76. Bruce, P.G., Freunberger, S.A., Hardwick, L.J., and Tarascon, J.-M. (2011). Li–O2 and Li–S batteries with high energy storage. Nat. Mater. *11*, 19–29. https://doi.org/10.1038/nmat3191.
77. Abraham, K.M., and Jiang, Z. (1996). A polymer electrolyte-based rechargeable lithium/oxygen battery. J. Electrochem. Soc. *143*, 1–5. https://doi.org/10.1149/1.1836378.
78. Aurbach, D., McCloskey, B.D., Nazar, L.F., and Bruce, P.G. (2016). Advances in understanding mechanisms underpinning lithium–air batteries. Nat. Energy *1*, 1–11. https://doi.org/10.1038/nenergy.2016.128.
79. Ogasawara, T., Débart, A., Holzapfel, M., Novák, P., and Bruce, P.G. (2006). Rechargeable Li2O2 electrode for lithium batteries. J. Am. Chem. Soc. *128*, 1390–1393. https://doi.org/10.1021/ja056811q.
80. Tarascon, J.-M., and Armand, M. (2001). Issues and challenges facing rechargeable lithium batteries. Nature *414*, 359–367. https://doi.org/10.1038/35104644.
81. Jeong, Y.S., Park, J.-B., Jung, H.-G., Kim, J., Luo, X., Lu, J., Curtiss, L., Amine, K., Sun, Y.-K., Scrosati, B., and Lee, Y.J. (2015). Study on the catalytic activity of noble metal nanoparticles on reduced graphene oxide for oxygen evolution reactions in lithium–air batteries. Nano Lett. *15*, 4261–4268. https://doi.org/10.1021/nl504425h.
82. Ma, J.-l., Meng, F.-l., Yu, Y., Liu, D.-p., Yan, J.-m., Zhang, Y., Zhang, X.-b., and Jiang, Q. (2019). Prevention of dendrite growth and volume expansion to give high-performance aprotic bimetallic Li-Na alloy–O_2 batteries. Nat. Chem. *11*, 64–70. https://doi.org/10.1038/s41557-018-0166-9.
83. Shen, Y., Sun, D., Yu, L., Zhang, W., Shang, Y., Tang, H., Wu, J., Cao, A., and Huang, Y. (2013). A high-capacity lithium–air battery with Pd modified carbon nanotube sponge cathode working in regular air. Carbon *62*, 288–295. https://doi.org/10.1016/j.carbon.2013.05.066.
84. Kim, S.H., Lee, Y.J., Kim, D.H., and Lee, Y.J. (2018). Bimetallic metal–organic frameworks as efficient cathode catalysts for Li–O_2 batteries. ACS Appl. Mater. Interfaces *10*, 660–667. https://doi.org/10.1021/acsami.7b15499.
85. Yan, W., Guo, Z., Xu, H., Lou, Y., Chen, J., and Li, Q. (2017). Downsizing metal–organic frameworks with distinct morphologies as cathode materials for high-capacity Li–O_2 batteries. Mater. Chem. Front. *1*, 1324–1330. https://doi.org/10.1039/C6QM00338A.
86. Yuan, M., Wang, R., Fu, W., Lin, L., Sun, Z., Long, X., Zhang, S., Nan, C., Sun, G., Li, H., and Ma, S. (2019). Ultrathin two-dimensional metal–organic framework nanosheets with the inherent open active sites as electrocatalysts in aprotic Li–O_2 batteries. ACS Appl. Mater. Interfaces *11*, 11403–11413. https://doi.org/10.1021/acsami.8b21808.
87. Hu, X., Zhu, Z., Cheng, F., Tao, Z., and Chen, J. (2015). Micro-nano structured Ni-MOFs as high-performance cathode catalyst for rechargeable Li–O_2 batteries. Nanoscale *7*, 11833–11840. https://doi.org/10.1039/C5NR02487K.
88. Wu, D., Guo, Z., Yin, X., Pang, Q., Tu, B., Zhang, L., Wang, Y.G., and Li, Q. (2014). Metal–organic frameworks as cathode materials for Li–O_2 batteries. Adv. Mater. *26*, 3258–3262. https://doi.org/10.1002/adma.201305492.
89. Li, N., Chang, Z., Zhong, M., Fu, Z.-X., Luo, J., Zhao, Y.-F., Li, G.-B., and Bu, X.-H. (2021). Functionalizing MOF with redox-active tetrazine moiety for improving the performance as cathode of Li–O_2 batteries. CCS Chem. *3*, 1297–1305. https://doi.org/10.31635/ccschem.020.202000284.
90. Zhang, X., Dong, P., Lee, J.-I., Gray, J.T., Cha, Y.-H., Ha, S., and Song, M.-K. (2019). Enhanced cycling performance of rechargeable Li–O_2 batteries via LiOH formation and decomposition using high-performance MOF-74@ CNTs hybrid catalysts. Energy Storage Mater. *17*, 167–177. https://doi.org/10.1016/j.ensm.2018.11.014.
91. Li, Y., and Dai, H. (2014). Recent advances in zinc–air batteries. Chem. Soc. Rev. *43*, 5257–5275. https://doi.org/10.1039/C4CS00015C.
92. Gu, Y., Chen, S., Ren, J., Jia, Y.A., Chen, C., Komarneni, S., Yang, D., and Yao, X. (2018). Electronic structure tuning in Ni_3FeN/r-GO aerogel toward bifunctional electrocatalyst for overall water splitting. ACS Nano *12*,

245–253. https://doi.org/10.1021/acsnano.7b05971.
93. Zhang, J., Zhao, Z., Xia, Z., and Dai, L. (2015). A metal-free bifunctional electrocatalyst for oxygen reduction and oxygen evolution reactions. Nat. Nanotechnol. *10*, 444–452. https://doi.org/10.1038/nnano.2015.48.
94. Li, Y., Gong, M., Liang, Y., Feng, J., Kim, J.-E., Wang, H., Hong, G., Zhang, B., and Dai, H. (2013). Advanced zinc-air batteries based on high-performance hybrid electrocatalysts. Nat. Commun. *4*, 1805. https://doi.org/10.1038/ncomms2812.
95. Wang, J., Wu, H., Gao, D., Miao, S., Wang, G., and Bao, X. (2015). High-density iron nanoparticles encapsulated within nitrogen-doped carbon nanoshell as efficient oxygen electrocatalyst for zinc–air battery. Nano Energy *13*, 387–396. https://doi.org/10.1016/j.nanoen.2015.02.025.
96. Prabu, M., Ketpang, K., and Shanmugam, S. (2014). Hierarchical nanostructured NiCo 2 O 4 as an efficient bifunctional non-precious metal catalyst for rechargeable zinc–air batteries. Nanoscale *6*, 3173–3181. https://doi.org/10.1039/C3NR05835B.
97. Shinde, S.S., Lee, C.H., Jung, J.-Y., Wagh, N.K., Kim, S.-H., Kim, D.-H., Lin, C., Lee, S.U., and Lee, J.-H. (2019). Unveiling dual-linkage 3D hexaiminobenzene metal–organic frameworks towards long-lasting advanced reversible Zn–air batteries. Energy Environ. Sci. *12*, 727–738. https://doi.org/10.1039/C8EE02679C.
98. Li, W., Wu, C., Ren, H., Fang, W., Zhao, L., and Dinh, K.N. (2020). Hybrid Cobalt and Iron Based Metal Organic Framework Composites as Efficient Bifunctional Electrocatalysts towards Long-Lasting Flexible Zinc-Air Batteries. Batter. Supercaps *3*, 1321–1328. https://doi.org/10.1002/batt.202000163.
99. Xiao, Y., Guo, B., Zhang, J., Hu, C., Ma, R., Wang, D., and Wang, J. (2020). A bimetallic MOF@ graphene oxide composite as an efficient bifunctional oxygen electrocatalyst for rechargeable Zn–air batteries. Dalton Trans. *49*, 5730–5735. https://doi.org/10.1039/D0DT00976H.
100. Liu, K., Huang, X., Wang, H., Li, F., Tang, Y., Li, J., and Shao, M. (2016). Co_3O_4–CeO_2/C as a highly active electrocatalyst for oxygen reduction reaction in Al–air batteries. ACS Appl. Mater. Interfaces *8*, 34422–34430. https://doi.org/10.1021/acsami.6b12294.
101. Liu, Y., Sun, Q., Li, W., Adair, K.R., Li, J., and Sun, X. (2017). A comprehensive review on recent progress in aluminum–air batteries. Green Energy Environ. *2*, 246–277. https://doi.org/10.1016/j.gee.2017.06.006.
102. Wang, X., Sebastian, P., Smit, M.A., Yang, H., and Gamboa, S. (2003). Studies on the oxygen reduction catalyst for zinc–air battery electrode. J. Power Sources *124*, 278–284. https://doi.org/10.1016/S0378-7753(03)00737-7.
103. Yang, S., and Knickle, H. (2002). Design and analysis of aluminum/air battery system for electric vehicles. J. Power Sources *112*, 162–173. https://doi.org/10.1016/S0378-7753(02)00370-1.
104. Cheng, F., and Chen, J. (2012). Metal–air batteries: from oxygen reduction electrochemistry to cathode catalysts. Chem. Soc. Rev. *41*, 2172–2192. https://doi.org/10.1039/C1CS15228A.
105. Mori, R. (2017). Electrochemical properties of a rechargeable aluminum–air battery with a metal–organic framework as air cathode material. RSC Adv. *7*, 6389–6395. https://doi.org/10.1039/C6RA25164A.
106. Manthiram, A., Fu, Y., Chung, S.-H., Zu, C., and Su, Y.-S. (2014). Rechargeable lithium–sulfur batteries. Chem. Rev. *114*, 11751–11787. https://doi.org/10.1021/cr500062v.
107. Manthiram, A., Chung, S.H., and Zu, C. (2015). Lithium–sulfur batteries: progress and prospects. Adv. Mater. *27*, 1980–2006. https://doi.org/10.1002/adma.201405115.
108. Wu, F., Ye, Y., Chen, R., Qian, J., Zhao, T., Li, L., and Li, W. (2015). Systematic effect for an ultralong cycle lithium–sulfur battery. Nano Lett. *15*, 7431–7439. https://doi.org/10.1021/acs.nanolett.5b02864.
109. Suriyakumar, S., and Stephan, A.M. (2020). Mitigation of polysulfide shuttling by interlayer/permselective separators in lithium–sulfur batteries. ACS Appl. Energy Mater. *3*, 8095–8129. https://doi.org/10.1021/acsaem.0c01354.
110. Liu, D., Zhang, C., Zhou, G., Lv, W., Ling, G., Zhi, L., and Yang, Q.H. (2018). Catalytic effects in lithium–sulfur batteries: promoted sulfur transformation and reduced shuttle effect. Adv. Sci. *5*, 1700270. https://doi.org/10.1002/advs.201700270.
111. Hong, X.-J., Song, C.-L., Yang, Y., Tan, H.-C., Li, G.-H., Cai, Y.-P., and Wang, H. (2019). Cerium based metal–organic frameworks as an efficient separator coating catalyzing the conversion of polysulfides for high performance lithium–sulfur batteries. ACS Nano *13*, 1923–1931. https://doi.org/10.1021/acsnano.8b08155.
112. Tao, X., Wang, J., Liu, C., Wang, H., Yao, H., Zheng, G., Seh, Z.W., Cai, Q., Li, W., Zhou, G., et al. (2016). Balancing surface adsorption and diffusion of lithium-polysulfides on nonconductive oxides for lithium–sulfur battery design. Nat. Commun. *7*, 11203. https://doi.org/10.1038/ncomms11203.
113. Shi, Z., Yang, Y., Huang, Y., Yue, H., Cao, Z., Dong, H., Yin, Y., and Yang, S. (2019). Organic alkali metal salt derived three-dimensional N-doped porous carbon/carbon nanotubes composites with superior Li–S battery performance. ACS Sustain. Chem. Eng. *7*, 3995–4003. https://doi.org/10.1021/acssuschemeng.8b05305.
114. Bai, S., Liu, X., Zhu, K., Wu, S., and Zhou, H. (2016). Metal–organic framework-based separator for lithium–sulfur batteries. Nat. Energy *1*, 1–6. https://doi.org/10.1038/nenergy.2016.94.
115. Liang, X., Garsuch, A., and Nazar, L.F. (2015). Sulfur cathodes based on conductive MXene nanosheets for high-performance lithium–sulfur batteries. Angew. Chem. Int. Ed. Engl. *54*, 3907–3911. https://doi.org/10.1002/anie.201410174.
116. Bian, Z., Yuan, T., Xu, Y., Pang, Y., Yao, H., Li, J., Yang, J., and Zheng, S. (2019). Boosting Li–S battery by rational design of freestanding cathode with enriched anchoring and catalytic N-sites carbonaceous host. Carbon *150*, 216–223. https://doi.org/10.1016/j.carbon.2019.05.022.
117. Liu, J., Yang, T., Wang, D.-W., Lu, G.Q., Zhao, D., and Qiao, S.Z. (2013). A facile soft-template synthesis of mesoporous polymeric and carbonaceous nanospheres. Nat. Commun. *4*, 2798. https://doi.org/10.1038/ncomms3798.
118. Gao, G., Sun, X., and Wang, L.-W. (2020). An inverse vulcanized conductive polymer for Li–S battery cathodes. J. Mater. Chem. A *8*, 21711–21720. https://doi.org/10.1039/D0TA06537D.
119. Yin, L., Wang, J., Lin, F., Yang, J., and Nuli, Y. (2012). Polyacrylonitrile/graphene composite as a precursor to a sulfur-based cathode material for high-rate rechargeable Li–S batteries. Energy Environ. Sci. *5*, 6966–6972. https://doi.org/10.1039/C2EE03495F.
120. Evers, S., and Nazar, L.F. (2013). New approaches for high energy density lithium–sulfur battery cathodes. Acc. Chem. Res. *46*, 1135–1143. https://doi.org/10.1021/ar3001348.
121. Wei Seh, Z., Li, W., Cha, J.J., Zheng, G., Yang, Y., McDowell, M.T., Hsu, P.-C., and Cui, Y. (2013). Sulphur–TiO2 yolk–shell nanoarchitecture with internal void space for long-cycle lithium–sulphur batteries. Nat. Commun. *4*, 1331. https://doi.org/10.1038/ncomms2327.
122. Seh, Z.W., Yu, J.H., Li, W., Hsu, P.-C., Wang, H., Sun, Y., Yao, H., Zhang, Q., and Cui, Y. (2014). Two-dimensional layered transition metal disulphides for effective encapsulation of high-capacity lithium sulphide cathodes. Nat. Commun. *5*, 5017. https://doi.org/10.1038/ncomms6017.
123. Zhang, N., Yang, Y., Feng, X., Yu, S.-H., Seok, J., Muller, D.A., and Abruña, H.D. (2019). Sulfur encapsulation by MOF-derived CoS_2 embedded in carbon hosts for high-performance Li–S batteries. J. Mater. Chem. A *7*, 21128–21139. https://doi.org/10.1039/C9TA06947J.
124. Hong, X.-J., Tan, T.-X., Guo, Y.-K., Tang, X.-Y., Wang, J.-Y., Qin, W., and Cai, Y.-P. (2018). Confinement of polysulfides within bi-functional metal–organic frameworks for high performance lithium–sulfur batteries. Nanoscale *10*, 2774–2780. https://doi.org/10.1039/C7NR07118C.
125. Feng, Y., Zhang, Y., Du, G., Zhang, J., Liu, M., and Qu, X. (2018). Li_2S–Embedded copper metal–organic framework cathode with superior electrochemical performance for Li–S batteries. New J. Chem. *42*, 13775–13783. https://doi.org/10.1039/C8NJ02370K.
126. Wang, Z., Wang, B., Yang, Y., Cui, Y., Wang, Z., Chen, B., and Qian, G. (2015). Mixed-metal–organic framework with effective Lewis acidic sites for sulfur confinement in high-performance lithium–sulfur batteries. ACS Appl. Mater. Interfaces *7*, 20999–21004. https://doi.org/10.1021/acsami.5b07024.
127. Zeng, Q., Xu, L., Li, G., Zhang, Q., Guo, S., Lu, H., Xie, L., Yang, J., Weng, J., Zheng, C., and Huang, S. (2023). Integrating Sub-Nano Catalysts into Metal-Organic Framework toward Pore-Confined Polysulfides Conversion in Lithium-Sulfur Batteries. Adv. Funct. Mater. *33*, 2304619. https://doi.org/10.1002/adfm.202304619.
128. Shimizu, T., Wang, H., Matsumura, D., Mitsuhara, K., Ohta, T., and Yoshikawa, H. (2020). Porous Metal–Organic Frameworks Containing Reversible Disulfide Linkages as Cathode Materials for Lithium-Ion Batteries. ChemSusChem *13*, 2256–2263. https://doi.org/10.1002/cssc.201903471.
129. Liu, X., Wang, S., Wang, A., Wang, Z., Chen, J., Zeng, Q., Chen, P., Liu, W., Li, Z., and Zhang, L. (2019). A new cathode material synthesized by a thiol-modified metal–organic framework (MOF) covalently connecting sulfur for superior long-cycling stability in lithium–sulfur batteries. J. Mater. Chem. A *7*, 24515–24523. https://doi.org/10.1039/C9TA08043K.

130. Somjit, V., Thinsoongnoen, P., Waiprasoet, S., Pila, T., Pattanasattayavong, P., Horike, S., and Kongpatpanich, K. (2021). Processable UiO-66 metal–organic framework fluid gel and electrical conductivity of its nanofilm with sub-100 nm thickness. ACS Appl. Mater. Interfaces *13*, 30844–30852. https://doi.org/10.1021/acsami.1c07262.

131. Zhang, H., Zhao, W., Wu, Y., Wang, Y., Zou, M., and Cao, A. (2019). Dense monolithic MOF and carbon nanotube hybrid with enhanced volumetric and areal capacities for lithium–sulfur battery. J. Mater. Chem. A *7*, 9195–9201. https://doi.org/10.1039/C9TA00485H.

132. Fan, L., Wu, H., Wu, X., Wang, M., Cheng, J., Zhang, N., Feng, Y., and Sun, K. (2019). Fe-MOF derived jujube pit like Fe3O4/C composite as sulfur host for lithium-sulfur battery. Electrochim. Acta *295*, 444–451. https://doi.org/10.1016/j.electacta.2018.08.107.

133. Bao, W., Zhang, Z., Zhou, C., Lai, Y., and Li, J. (2014). Multi-walled carbon nanotubes@mesoporous carbon hybrid nanocomposites from carbonized multi-walled carbon nanotubes@ metal–organic framework for lithium sulfur battery. J. Power Sources *248*, 570–576. https://doi.org/10.1016/j.jpowsour.2013.09.132.